

Accepted Manuscript

Bacterial vs human sphingosine-1-phosphate lyase (S1PL) in the design of potential S1PL inhibitors

Pol Sanllehí, José Luis Abad, Josefina Casas, Jordi Bujons, Antonio Delgado

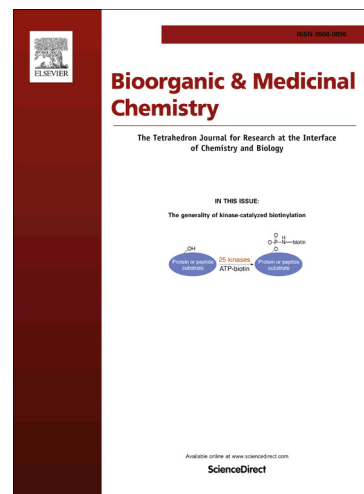
PII: S0968-0896(16)30540-5
DOI: <http://dx.doi.org/10.1016/j.bmc.2016.07.033>
Reference: BMC 13146

To appear in: *Bioorganic & Medicinal Chemistry*

Received Date: 24 May 2016
Revised Date: 13 July 2016
Accepted Date: 16 July 2016

Please cite this article as: Sanllehí, P., Abad, J.L., Casas, J., Bujons, J., Delgado, A., Bacterial vs human sphingosine-1-phosphate lyase (S1PL) in the design of potential S1PL inhibitors, *Bioorganic & Medicinal Chemistry* (2016), doi: <http://dx.doi.org/10.1016/j.bmc.2016.07.033>

This is a PDF file of an unedited manuscript that has been accepted for publication. As a service to our customers we are providing this early version of the manuscript. The manuscript will undergo copyediting, typesetting, and review of the resulting proof before it is published in its final form. Please note that during the production process errors may be discovered which could affect the content, and all legal disclaimers that apply to the journal pertain.



Bacterial vs human sphingosine-1-phosphate lyase (S1PL) in the design of potential S1PL inhibitors

Pol Sanllehí,^{[a][b]} José Luis Abad,^[a] Josefina Casas,^[a] Jordi Bujons,^{*[c]} and Antonio Delgado^{*[a][b]}

[a] Institute for Advanced Chemistry of Catalonia (IQAC-CSIC), Research Unit on Bioactive Molecules; Department of Biomedical Chemistry, Jordi Girona 18-26; E-08034 Barcelona (Spain)

[b] University of Barcelona (UB); Faculty of Pharmacy; Department of Pharmacology, Toxicology and Medicinal Chemistry; Unit of Pharmaceutical Chemistry (Associated Unit to CSIC); Avda. Joan XXIII s/n, E-08028 Barcelona (Spain)

[c] Institute for Advanced Chemistry of Catalonia (IQAC-CSIC), Department of Biological Chemistry and Molecular Modeling, Jordi Girona 18-26, E-08034 Barcelona (Spain)

Abstract

A series of potential active-site sphingosine-1-phosphate lyase (S1PL) inhibitors have been designed from scaffolds **1** and **2**, arising from virtual screening using the X-ray structures of the bacterial (StS1PL) and the human (hS1PL) enzymes. Both enzymes are very similar at the active site, as confirmed by the similar experimental kinetic constants shown by the fluorogenic substrate **RBM13** in both cases. However, the docking scoring functions used probably overestimated the weight of electrostatic interactions between the ligands and key active-site residues in the protein environment, which may account for the modest activity found for the designed inhibitors. In addition, the possibility that the inhibitors do not reach the enzyme active site should not be overlooked. Finally, since both enzymes show remarkable structural differences at the access channel and in the proximity to the active site cavity, caution should be taken when designing inhibitors acting around that area, as evidenced by the much lower activity found in StS1PL for the potent hS1PL inhibitor **D**.

Keywords: sphingolipids; lyase; inhibitors; design; docking

Introduction

Sphingosine-1-phosphate lyase (S1PL) is a key enzyme of sphingolipid (SL) catabolism that catalyzes the irreversible degradation of sphingosine-1-phosphate (S1P) into phosphoethanolamine (PEA) and (*E*)-hexadecenal in the endoplasmic reticulum (ER).¹ Together with sphingosine-1-phosphate phosphatase (S1PP), S1PL regulates the levels of S1P and contributes to the so-called “sphingolipid rheostat”, a system that controls cell fate based on the ratio of intracellular proliferative S1P and the apoptogenic sphingosine (So) and ceramide (Cer).^{2,3}

Some functional S1PL inhibitors have been reported in the literature (Figure 1). 4-Deoxy pyridoxine (DOP) is a non-selective inhibitor of PLP-dependent enzymes,^{4,5} whereas THI and related second-generation analogs are regarded as functional S1PL antagonists, whose activity has been attributed to their interference with vitamin B₆.⁶⁻⁸ Concerning competitive S1PL inhibitors, phosphonate A (K_i = 5 μM) (Figure 1), showed properties of being a tight substrate binder,⁹ whereas the S1P receptor agonist FTY-720¹⁰ (Figure 1) also inhibits S1PL, although at around 100-fold higher concentration (52.4 μM)¹¹ than that required for (*S*)-FTY720 phosphate for direct S1P agonism.¹² In the last years, the development of HTS programs has led to some interesting hits as S1PL inhibitors. For example, in the library developed by Lexicon, compound B (Figure 1) showed high inhibition in cellular assays (IC₅₀ = 2.1 μM), which was not reproduced in vivo.^{6,13} More recently, researchers at Novartis reported on the potent piperazinophthalazine derivatives **C**¹⁴ and **D**¹⁵ (Figure 1) as S1PL inhibitors with IC₅₀ values of 210 nM and 24 nM, respectively. In the course of this work, a recent HTS program has led to the discovery of compound **E**, as a new hS1PL inhibitor (IC₅₀ = 230 nM) in a cell assay.¹⁶ Likewise, several S1PL potential inhibitors based on a virtual screening approach, have been suggested.¹⁷

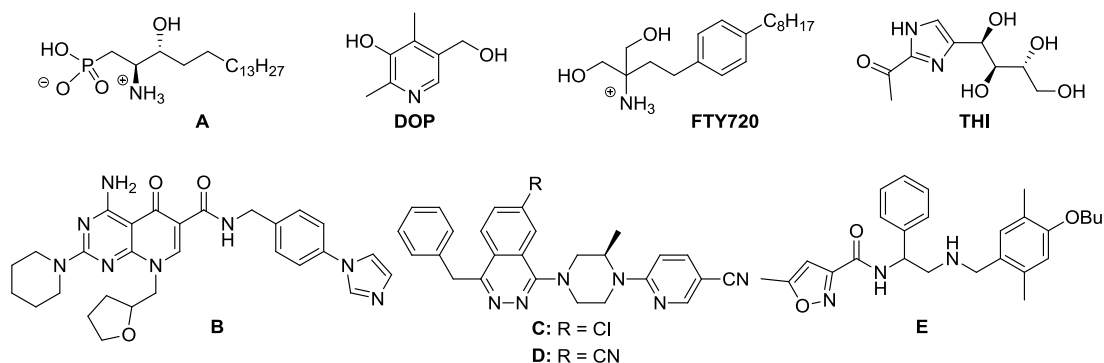


Figure 1. Some of the most representative S1PL inhibitors reported in the literature.

From a mechanistic standpoint, S1PL belongs to the superfamily of PLP (pyridoxal 5'-phosphate)-dependent enzymes. The enzyme is located in the ER and possesses an *N*-terminal luminal domain, a transmembrane segment and a soluble PLP-binding domain, responsible for the catalytic activity.¹⁸ The enzyme is active as an intertwined dimer with two active sites.^{19,20} The recombinant human enzyme (hS1PL) has been expressed in *E.coli*²¹ and, more efficiently, in Sf9 insect cells.¹⁵ The crystal structures of yeast S1PL and that of a putative prokaryotic homolog from *Symbiobacterium thermophilum* (StS1PL) were reported and used to generate a reliable homology model of the human enzyme that allowed the identification of the key residues involved in S1P cleavage.¹⁹ More recently, a co-crystal of the human recombinant enzyme with a bound selective inhibitor has also been reported.¹⁵ Interestingly, the structure of this hS1PL showed a high sequence and structural similarity with those of previously reported homologues.²⁰ Based on the high similarity between the X-ray structures of hS1PL¹⁵ and that of the bacterial homologue StS1PL,¹⁹ we envisaged the structure-based design of potential S1PL active site-directed inhibitors. For that purpose we performed a virtual screening study against both enzymes with the goal of identifying structural features to build a common pharmacophore that guide the design of new potential S1PL binders. As a result, a small collection of compounds has been designed, synthesized and tested on both hS1PL and StS1PL enzymes. In addition, we have also compared both enzymes against our fluorogenic substrate **RBM13**²² and the potent inhibitor **D** (Figure 1). The results of these studies, together with the determination of the kinetic constants for **RBM13** in purified hS1PL and StS1PL, are reported in this paper.

Results and discussion

1. Library design

Comparison of the active site structures from StS1PL (PDB 3MAD)¹⁹ and hS1PL (PDB 4Q6R)¹⁵ revealed a high level of sequence and structural similarity (Figures S1 and S2). Thus, from 30 residues that conform their active site cavity and access channel, 26 are identical and 3 are conserved in both proteins, and the RMSD among the C_α-atoms of these residues is only 0.71 Å. This suggested that StS1PL could be a good active site protein model for the discovery of hS1PL inhibitors.

A database of about 650000 lead-like commercial chemical structures²³ was virtually screened against StS1PL and hS1PL to find potential active site binders. For that purpose, a virtual screening workflow²⁴ that uses the docking software Glide²⁵⁻²⁸ to perform the flexible docking of the compounds at different levels of accuracy was employed. The results of this virtual screening showed that ionized carboxylic acids that bind at, or close to, an anion binding site near to the PLP cofactor (Figures S3 and S4, Charts S1-S4) were among the best scored hits for both targets. This site is formed by residues Y105, H129 and K317 of StS1PL, which correspond to Y150, H174 and K359 in hS1PL, and it has been postulated as the binding site for the phosphate group of the natural substrate S1P.¹⁹ This was not surprising, since carboxylate is a well-known phosphate surrogate.²⁹ In addition to the carboxylate group, many of these compounds also showed, as a common feature, the presence of a variable moiety that links the carboxylate group to an aromatic ring, which, in turn, is decorated with one or more variable substituents (Figure 2 and Charts S1-S4). The linker moiety was of variable nature, mostly formed by a short linear chain (e.g. -CH₂O-), although longer chains with different functionalities (e.g. amide groups) were also found. This suggested that the binding site for the aromatic group of the hits is not in a well delimited region, but rather in a relatively large hydrophobic patch formed by residues L128, H129, Y249, W340 and Y345 of StS1PL, which correspond to L173, H174, F290, W382 and Y387 of hS1PL, respectively. Finally, the variable region decorating the aromatic ring included, in most cases, one or more additional aromatic rings, which occupied the same protein region as the known S1PL inhibitor **C**¹⁵ (Figure 1).

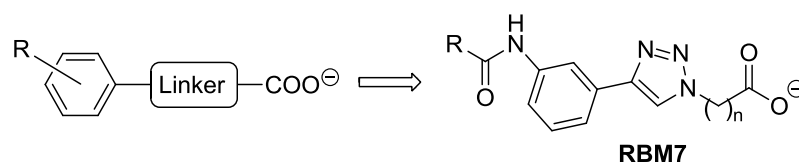
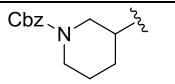
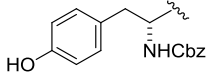
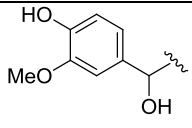
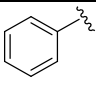
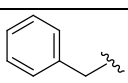


Figure 2. General structure of the putative S1PL ligands and derived scaffold structure **RBM7**, as detected by virtual screening, and constituted by a carboxylate group, a linker and a substituted aromatic ring.

Taking into account the above features, we proposed **RBM7** as a suitable scaffold to develop a small library of potential S1PL binders. In this structure, the triazole central core was chosen as part of the linker for its synthetic availability, since it can be easily assembled using standard click chemistry protocols based on alkyne-azide cycloadditions. Furthermore, by binding to the phenyl ring, it would provide an extended aromatic region able to establish strong interactions with the aromatic residues present in the above mentioned receptor hydrophobic patch. On the other hand, an amide group bound to the phenyl ring would allow the exploration of a diversity of R-substituents, coming from suitable carboxylic acid precursors, which would interact with the more external part of the channel that leads to the active site cavity of S1PL. A virtual library of compounds with the general structure **RBM7** was enumerated starting from a diverse collection of 6048 commercial carboxylic acids (R-COOH), which were combined *in silico* with scaffolds **1** and **2** (Scheme 1), to yield a final library of about 12000 compounds. This library was docked against StS1PL and hS1PL using Glide XP.²⁷ To refine their structures and docking scores, a further induced fit docking protocol³⁰⁻³² was applied to some of the best poses determined. Based on their scores, the diversity of their structures and other practical criteria, like synthetic suitability or commercial availability, 12 virtual hits were selected for synthesis (see Table 1 and Charts S5 and S6 for docking scores). These virtual hits showed similar binding modes (Figures S5-S10), with their carboxylate groups located at the anion binding site and the central triazole and phenyl rings interacting with the residues of the hydrophobic patch of each protein, in many cases through π -stacking interactions.

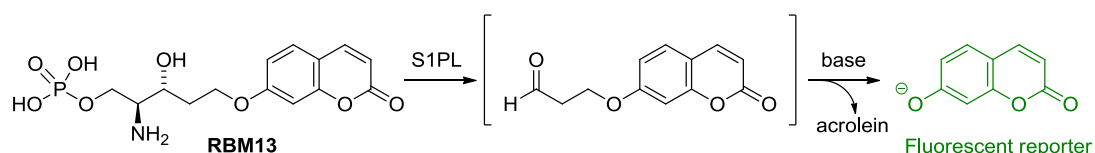
RBM7-47		1	35
RBM7-48		2	29
RBM7-49		2	65
RBM7-66		2	51
RBM7-67		2	50

(a) Overall yield (from starting bromoesters, see Experimental and Scheme 1)

3. Inhibition studies on StS1PL and hS1PL

3.1. Optimization of the inhibition assay

Among the several assays reported for the determination of S1PL activity,^{33,34} those amenable to “on-plate” analysis are particularly interesting for their application to HTS protocols. In this context, some time ago we developed the fluorogenic probe **RBM13**,²² a S1PL substrate that affords the fluorescent reporter umbelliferone, after base-promoted decomposition of the intermediate aldehyde product (Scheme 2).



Scheme 2. Generation of the umbelliferone reporter from **RBM13**

So far, the only kinetic constants for **RBM13** have been determined in cell lysates of murine embryonic fibroblasts.²² In this work, these parameters have also been determined in purified StS1PL and hS1PL, which required a thorough protocol optimization (Figure 3). StS1PL was expressed and purified following an adapted version of a reported protocol¹⁹ (see Supporting Information). Initially, **RBM13** was tested as StS1PL substrate at 62 μM , in

agreement with the above protocol. Incubation of **RBM13** with different amounts of StS1PL showed linearity in product formation up to 50 $\mu\text{g}/\text{mL}$ StS1PL (Figure 3A). The optimal enzyme concentration was fixed at 25 $\mu\text{g}/\text{mL}$, in which 12 % of the substrate was metabolized, with a 12-fold increase of the fluorescence signal with respect to the blank. Product formation was also time-dependent, since the amount of umbelliferone increased linearly up to 90 min (Figure 3B). From these results, an incubation time of 60 min was considered suitable for further assays. Kinetic parameters for **RBM13** against StS1PL were thus determined (Figure 3C) as $K_M = 1522 \pm 73 \mu\text{M}$ and $V_{\max} = 46 \pm 2 \text{ pmol}\cdot\text{min}^{-1}\cdot\mu\text{g}^{-1}$ ($V_{\max}/K_M = 0.03 \pm 0.002$). Concerning hS1PL, the ability of **RBM13** as substrate was also evidenced, as shown in Figure 3D. At 3 $\mu\text{g}/\text{mL}$ of hS1PL (corresponding to a 2% substrate conversion) a 4-fold increase in the fluorescence signal was observed with respect to a blank experiment without enzyme. Under these conditions, product formation increased linearly up to 2 h of incubation time (Figure 3E). Hence, an incubation time of 60 min was considered suitable. The reaction rate was dependent on the substrate concentration (Figure 3E), with $K_M = 1994 \pm 121 \mu\text{M}$ and $V_{\max} = 107 \pm 11 \text{ pmol}\cdot\text{min}^{-1}\cdot\mu\text{g}^{-1}$ ($V_{\max}/K_M = 0.05 \pm 0.006$). Since the determined kinetic parameters were in the same order of magnitude for both bacterial and human enzymes, a similar behaviour of **RBM13** towards both enzyme sources can be inferred.

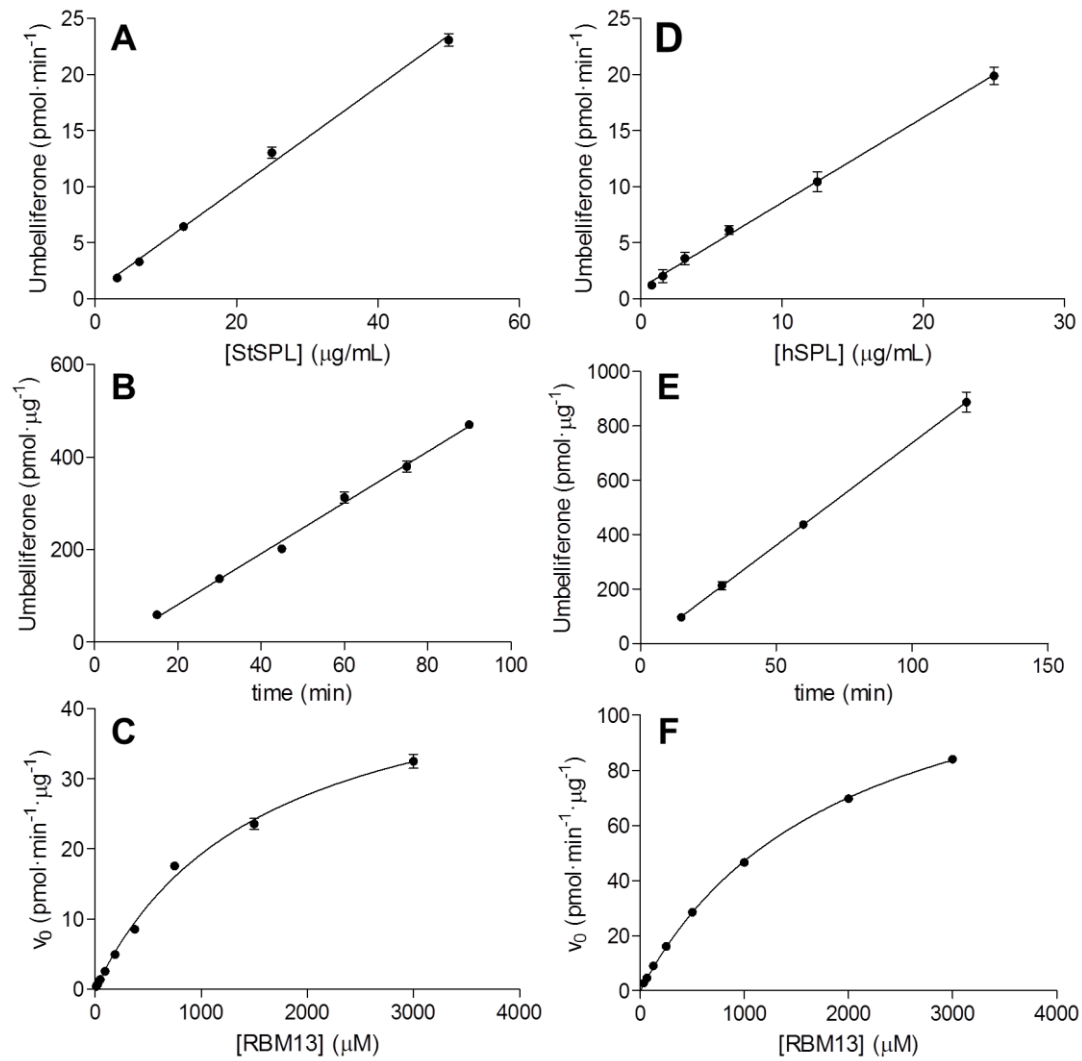


Figure 3. Enzyme concentration (A, D) and time-dependence (B, E) of the S1PL reaction using **RBM13** as substrate against StS1PL (A,B) and hS1PL (D,E). Substrate concentration was $62 \mu\text{M}$ (A,B) and $125 \mu\text{M}$ (D,E). In A and D, incubation time was 60 min. Enzyme concentration was $25 \mu\text{g}/\text{mL}$ (B) and $3 \mu\text{g}/\text{mL}$ (E). Substrate concentration dependence of the StS1PL reaction (C) and the hS1PL reaction (F) using **RBM13** as substrate at graded concentrations. In both cases, the substrate was incubated for 60 min with $25 \mu\text{g}/\text{mL}$ (C) or $3 \mu\text{g}/\text{mL}$ (F) of StS1PL and hS1PL, respectively. Data correspond to one representative experiment performed twice (with triplicates).

3.2. Activity of compounds **RBM7** as StS1PL and hS1PL inhibitors

Using **RBM13** as fluorogenic substrate, carboxylates **RBM7** (Table 1) were evaluated as S1PL inhibitors at 250 μM in both enzyme sources. The recently reported potent and selective hS1PL inhibitor **D**¹⁵ (Figure 1), was also included in this study as positive control of inhibition. The results are collected in Figure 4. Carboxylates **RBM7** showed activities ranging from low to moderate against both enzyme sources. In the case of hS1PL, only carboxylates **RBM7-42**, **RBM7-43**, **RBM7-44**, **RBM7-45** and **RBM7-48** exerted significant inhibition. Compound **RBM7-43** was the most active compound of this series with a 33 % inhibition. In contrast, compounds **RBM7-31**, **RBM7-44**, **RBM7-47**, **RBM7-48**, and **RBM7-49** showed significant inhibition of StS1PL, being carboxylate **RBM7-48** the most active compound of this series (31 % of inhibition). Comparison of activities for compounds **RBM7** showed small differences on their behavior against each enzyme source. Only **RBM7-43** showed a significant selectivity towards hS1PL ($P < 0.001$; unpaired two-tailed t-test; $n = 6$). Conversely, **RBM7-48**, the most active against StS1PL, showed little selectivity. As expected, compound **D** behaved as a potent hS1PL inhibitor in our fluorogenic assay, with a residual enzyme activity of around 2 % at 10 μM (Figure 4) and $\text{IC}_{50} = 93.5 \pm 6.0 \text{ nM}$ (Figure S13B), consistent with the reported value.¹⁵ However, compound **D** turned out to be significantly less active against StS1PL ($P < 0.001$; unpaired two-tailed t-test; $n = 6$), even at an equimolar concentration with the substrate (125 μM). Under these conditions, only a moderate decrease on the StS1PL activity (around 34 %) was observed (Figure 4). This lower activity showed by compound **D** against StS1PL was unexpected. Nonetheless, this result was confirmed using a slightly modified version of a reported LC/MS method to measure enzyme activity with natural S1P as substrate.¹⁵ Briefly, S1PL activity in the presence of the inhibitor (50 μM) was determined using natural S1P (10 μM) as substrate and trapping the enzyme reaction product (*trans*-2-hexacenedal) as an isonicotinyldiazide, prior to LC/MS quantification. Under these conditions, compound **D** also behaved as a potent hS1PL inhibitor (97 % inhibition), while it only exerted a moderate 15 % inhibition on StS1PL, consistent with the results obtained in our fluorogenic assay (See Figure S13A).

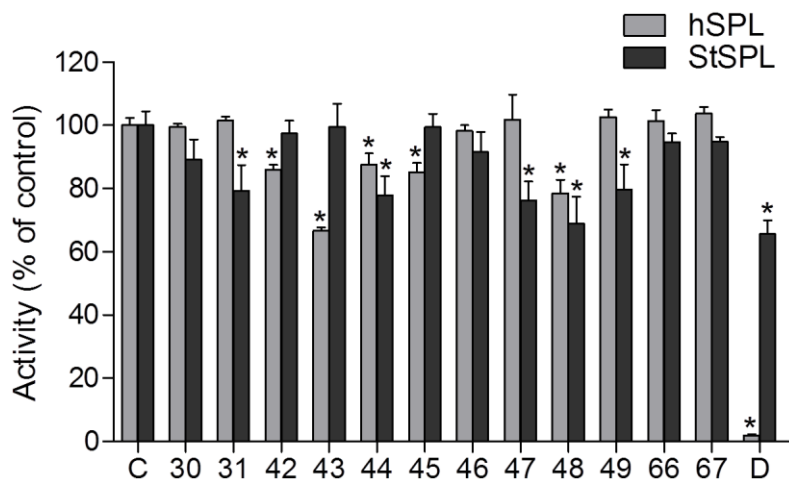


Figure 4. Activity (% of control) of hS1PL (3 µg/mL) and StS1PL (25 µg/mL) in the absence (C, control) or in the presence of compounds **RBM7** (indicated with the last two digits, for the sake of clarity) and compound **D** (taken as positive control of inhibition). Compounds were tested at 250 µM, except for compound **D**, which was tested at 10 µM (for hS1PL) and 125 µM (for StS1PL). In both cases, compound **RBM13** was used as substrate at a final concentration of 125 µM. Data are the mean \pm SD of two independent experiments with triplicates. Data were analyzed by one way ANOVA following by Dunnet's multiple comparison post-test if ANOVA $P < 0.05$. (*, $P < 0.001$ from control).

The different activity of inhibitor **D** against hS1PL and StS1PL can be explained on the basis of the structural differences between both proteins at the access channel and vestibule to the active site cavity. Superimposition of the surface of hS1PL on the structure of StS1PL shows a protrusion from the surface of several sidechain residues of the bacterial protein, in particular those of L344, F346 and L497 (Figure 5), in agreement with a very recent report.³⁵ This could preclude the binding of inhibitors **C** or **D** at that site, as we have experimentally observed for **D**. These structural differences between StS1PL and hS1PL should be taken into account if the more easily available StS1PL is taken as a model for the design of potential inhibitors targeting the S1PL access channel.^{16,35}

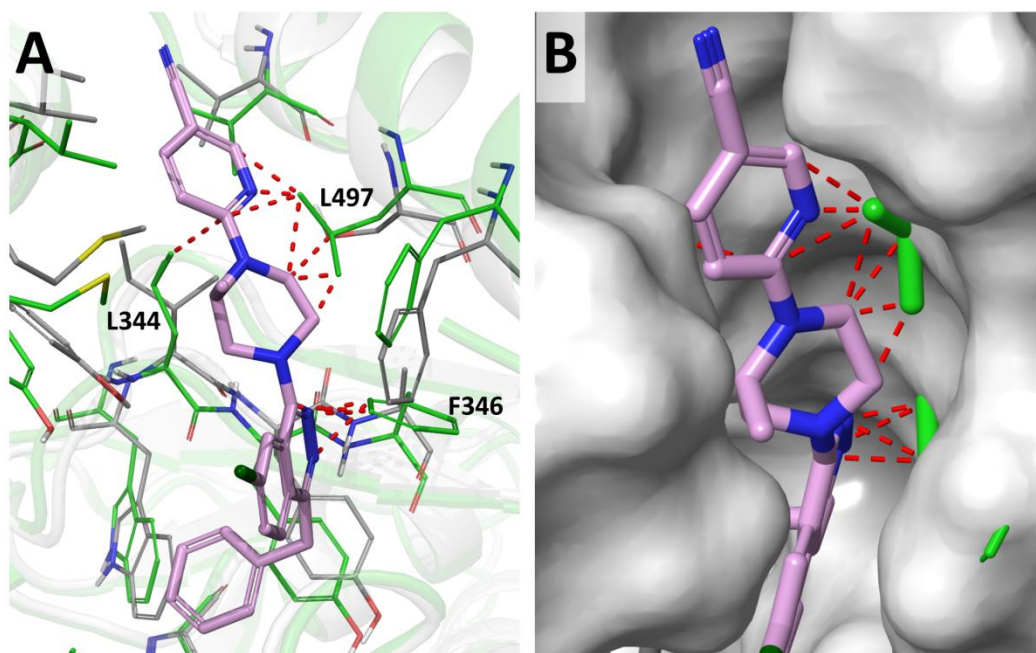


Figure 5. (A) Crystal structure of hS1PL (PDB 4Q6R, grey)¹⁵ with the bound inhibitor **C** (light purple) and superposed structure of StS1PL (PDB 3MAD, green).¹⁹ StS1PL residues L344, F346 and L497 (corresponding to I386, A388 and S542 of hS1PL) are labeled. (B) A close up view of the hS1PL surface (grey) at the inhibitor binding site and StS1PL residues (green) protruding from the surface. Red dashed lines indicate bad clashes between the StS1PL residues and a hypothetically bound inhibitor **C**.

Concerning the modest activity of compounds **RBM7** (Figure 4), a number of causes might explain the discrepancy with what was expected, based on the computational docking results. One concern is the ionization state of the carboxylate group present in our compounds and that of the ionizable protein residues at the anion binding site. Despite the fact that our virtual screening study considered two possibilities for the protonation state of the 3-hydroxypyridine and the imine moieties on the K359-PLP complex (in hS1PL) or K311-PLP complex (in StS1PL), the results obtained in both cases were similar (Charts S1-S4, Figures S3-S4). On the other hand, there are two additional residues at the anion binding site of both proteins that might be ionized, i.e. H129 and K317 of StS1PL or H174 and K359 of hS1PL. Our assumption was that these residues were in their ionic form, allowing the establishment of strong electrostatic and hydrogen bond interactions with the ligands. This assumption is probably right when the anion is a phosphate group (either from the buffer or

that present in the natural substrate S1P), and it seemed also reasonable for a carboxylate group, since there is in fact one molecule of citric acid bound at the same site in the crystal structure of hS1PL (PDB 4Q6R).¹⁵ However, the fact that compounds **RBM7** could be less acidic than expected in the protein environment should not be disregarded, thus precluding the interaction with the protein in their anionic form. Similarly, it is conceivable that the histidine residue at the anion binding site could be in its neutral state if there is not a strongly anionic bound ligand. This could have led to an overestimation of the potency of the polar interactions between the ligands and the proteins. Moreover, scoring functions in docking software are usually too crude to rank ligands according to their binding potency³⁶ and results arising only from docking estimates should be taken with caution.¹⁷ In addition, the possibility that the inhibitors do not reach the enzyme active site should not be overlooked. In any case, a strong structural similarity between hS1PL and its bacterial surrogate at the active site can be inferred from structural data and also by the similar biochemical parameters found for our fluorogenic substrate **RBM13** (see above). This justifies the use of the more easily available bacterial source when planning the design of active-site directed inhibitors, as we have observed in a series of substrate analogs.³⁷ However, more caution should be taken for inhibitors targeting the active site access channel, for which alternative chimeric constructs from bacterial origin represent interesting alternatives.³⁵

Conclusions

In summary, attempts to rationally design a set of active-site directed S1PL inhibitors using scaffold **RBM7** have met with limited success. Either overestimation of the ionic interactions in the active site or the inability of our compounds to reach it, may explain the observed results. On the other hand, the structural differences between StS1PL and hS1PL found at the access channel to the enzyme active site cavity can explain the lack of activity found for inhibitor **D** on StS1PL and questions the use of the more easily available StS1PL as template for the design of inhibitors acting on this access area. Finally, our previously reported fluorogenic probe **RBM13** was revealed as a suitable substrate for hS1PL, which widens the scope and the applicability of this substrate in this area of research.^{16,35}

Acknowledgments

Partial financial support from the “Ministerio de Economía y Competitividad”, Spain (Grant CTQ2014-54743-R) and “Fundació La Marató de TV3” (Grants 112130 and 112132) are acknowledged. We are also grateful to Dr. Andreas Billich (Novartis) for a generous gift of hS1PL and compound D, to Dr. Karel Hernández, for technical assistance in StS1PL expression and to Prof. Gemma Fabriàs for helpful discussions.

Supporting

Experimental protocols for compounds obtained from general procedures 2 and 3 and NMR data for all compounds.

Alignment of human (hS1PL), *Symbiobacterium thermophilum* (StS1PL) and *Saccharomyces cerevisiae* (ScS1PL) S1PL sequences and structures

Computational virtual screening methods and docking scores

Docked poses for compounds RMB7

Experimental

General

Unless otherwise stated, reactions were carried out under argon atmosphere. Dry solvents were obtained by passing through an activated alumina column on a Solvent Purification System (SPS). Commercially available reagents and solvents were used with no further purification. All reactions were monitored by TLC analysis using ALUGRAM[®] SIL G/UV₂₅₄ precoated aluminum sheets (Machery-Nagel). UV light was used as the visualizing agent and a 5% (w/v) ethanolic solution of phosphomolybdic acid as the developing agent. Flash column chromatography was carried out with the indicated solvents using flash-grade silica gel (37-70 mm). Preparative reversed-phase purifications were performed on a Biotage[®] Isolera[™] One equipment with the indicated solvents using a Biotage[®] SNAP cartridge (KP-C18-HS, 12 g) at a flow rate of 12 mL/min. Yields refer to chromatographically and spectroscopically pure compounds, unless otherwise stated.

NMR spectra were recorded at room temperature on a Varian Mercury 400 instrument. The chemical shifts (δ) are reported in ppm relative to the solvent signal, and coupling constants (J) are reported in Hertz (Hz). For $\text{CDCl}_3/\text{CD}_3\text{OD}$ solvent mixtures, chemical shifts are expressed relative to the residual peak of CD_3OD . The following abbreviations are used to define the multiplicities in ^1H NMR spectra: s = singlet, d = doublet, t = triplet, q = quartet, dd = doublet of doublets, ddd = doublet of doublet of doublets, m = multiplet, br = broad signal and app = apparent.

High Resolution Mass Spectrometry analyses were carried out on an Acquity UPLC system coupled to a LCT Premier orthogonal accelerated time-of-flight mass spectrometer (Waters) using electrospray ionization (ESI) technique.

All biochemical reagents were commercially available and were used without further purification. **RBM13**, S1P and pentadecanal were synthesized in our laboratories following previously described methods.^{22,38,39}

General Synthetic Methods

General procedure 1: Copper-catalyzed cycloaddition between 3-ethynylaniline and azides **3** and **4**

To a solution of 3-ethynylaniline (1.5 mL, 1.56 g, 13.3 mmol) and the azide **3** or **4** (1.2 eq/mol) in a mixture $\text{H}_2\text{O}/\text{THF}$ (1:1) (75 mL), $\text{CuSO}_4 \cdot 5\text{H}_2\text{O}$ (0.1 eq.) and sodium ascorbate (0.1 eq.) were added. After stirring under argon at rt for 1 h, the reaction mixture was extracted with EtOAc (3 x 50 mL). The combined organic layers were dried over anhydrous MgSO_4 and concentrated to give a residue which was purified by flash chromatography on elution with DCM/MeOH (98.5:1.5) to afford the corresponding cycloaddition adducts.

Methyl 2-(4-(3-aminophenyl)-1H-1,2,3-triazol-1-yl)acetate (**1**)

Compound **1** (pale yellow solid, 3.72 g, quantitative yield) was obtained from 3-ethynylaniline (1.8 mL, 16.0 mmol), azide **RBM7-019** (2.21 g, 19.2 mmol), $\text{CuSO}_4 \cdot 5\text{H}_2\text{O}$ (399 mg, 1.6 mmol) and sodium ascorbate (317 mg, 1.6 mmol), according to general procedure 1.

^1H NMR (400 MHz, CDCl_3) δ 7.86 (s, 1H), 7.29 – 7.27 (m, 1H), 7.23 – 7.14 (m, 2H), 6.68 (ddd, $J = 7.7, 2.4, 1.2$ Hz, 1H), 5.21 (s, 2H), 3.83 (s, 3H).

^{13}C NMR (101 MHz, CDCl_3) δ 166.9, 148.4, 146.8, 131.3, 129.9, 121.2, 116.3, 115.3, 112.5, 53.2, 50.9.

HRMS calcd. for $\text{C}_{11}\text{H}_{13}\text{N}_4\text{O}_2$ ($[\text{M} + \text{H}]^+$): 233.1039, found: 233.1037.

Methyl 3-(4-(3-aminophenyl)-1H-1,2,3-triazol-1-yl)propionate (2)

Compound **2** (pale yellow solid, 2.54 g, 97%) was obtained from 3-ethynylaniline (1.2 mL, 10.7 mmol), azide **RBM7-020** (1.65 g, 12.8 mmol), $\text{CuSO}_4 \cdot 5\text{H}_2\text{O}$ (266 mg, 1.1 mmol) and sodium ascorbate (211 mg, 1.1 mmol), according to general procedure 1.

^1H NMR (400 MHz, CDCl_3) δ 7.82 (s, 1H), 7.26 – 7.25 (m, 1H), 7.22 – 7.12 (m, 2H), 6.66 (ddd, $J = 7.8, 2.4, 1.2$ Hz, 1H), 4.69 (t, $J = 6.4$ Hz, 2H), 3.71 (s, 3H), 3.01 (t, $J = 6.4$ Hz, 2H).

^{13}C NMR (101 MHz, CDCl_3) δ 171.2, 147.9, 146.9, 131.5, 129.8, 120.7, 116.1, 115.1, 112.4, 52.3, 45.6, 34.6.

HRMS calcd. for $\text{C}_{12}\text{H}_{15}\text{N}_4\text{O}_2$ ($[\text{M} + \text{H}]^+$): 247.1195, found: 247.1188.

General procedure 2: HATU-mediated coupling between 1 or 2 and carboxylic acids.

In a typical run, a 15 mL screw cap tube was charged with the selected carboxylic acid (0.5 mmol), HATU (2 eq/mol), DMF (1 mL) and DIPEA (2 eq/mol.). A solution of **1** or **2** (0.5 mmol) in DMF (1 mL) was then added dropwise. The tube was flushed with argon, sealed, and the mixture was stirred overnight at 40 °C. After cooling down to rt, the crude reaction mixture was diluted with water (10 mL) and extracted with EtOAc (3 x 15 mL). The combined organic layers were washed with brine (3 x 15 mL), dried over anhydrous MgSO_4 , filtered and concentrated under reduced pressure to give a residue, which was purified as indicated for each compound. (see Supporting Material).

General procedure 3: EDC/HOBt-mediated coupling for amide-bond formation.

To a stirred solution of the selected carboxylic acid (0.5 mmol) and HOBt (1.2 eq/mol) in DMF, was added dropwise a solution of aniline **2** (0.5 mmol.) in DMF. EDC (1.2 eq/mol) was then added portionwise and the mixture was stirred overnight at rt. The crude reaction mixture was diluted with water (10 mL) and extracted with EtOAc (3 x 15 mL). The combined

organic layers were washed with brine (3 x 15 mL), dried over anhydrous MgSO₄, filtered and concentrated under reduced pressure to give a residue, which was purified as indicated for each compound in the Supporting Material.

General procedure 4: base-mediated hydrolysis of methyl esters.

To a stirred solution of the starting methyl ester (0.05 mmol) in THF/H₂O (3:1) (20 mL), LiOH (3 eq/mmol.) was added at 0 °C. After stirring at the same temperature for 1.5 h, the reaction mixture was acidified with aqueous 1N HCl and extracted with EtOAc (3 x 15 mL). The combined organic layers were dried over anhydrous MgSO₄, filtered and concentrated under reduced pressure to give a residue, which, unless otherwise noted, was purified by preparative RP chromatography using 0.2 % formic acid in acetonitrile (A) and 0.2 % aq. formic acid (B) as solvents (from 5 to 100 % A in B).

(S)-3-(4-(3-(1-(2-(((benzyloxy)carbonyl)amino)acetyl)pyrrolidine-2-carboxamido)phenyl)-1H-1,2,3-triazol-1-yl)propanoic acid (RBM7-030)

Compound **RBM7-030** (white solid, 31 mg, 91 %) was obtained from methyl ester **RBM7-028** (35 mg, 0.066 mmol) and LiOH (5 mg, 0.196 mmol), according to general procedure 4.

¹H NMR (400 MHz, CD₃OD, major rotamer) δ 8.26 (s, 1H), 7.98 (t, *J* = 1.8 Hz, 1H), 7.60 – 7.51 (m, 1H), 7.42 – 7.22 (m, 6H), 5.09 (s, 2H), 4.69 (t, *J* = 6.6 Hz, 2H), 4.58 (dd, *J* = 8.3, 3.7 Hz, 2H), 4.02 (app q, *J* = 17.1 Hz, 2H), 3.74 – 3.66 (m, 1H), 3.65 – 3.58 (m, 1H), 3.00 (t, *J* = 6.6 Hz, 2H), 2.32 – 2.21 (m, 1H), 2.19 – 1.92 (m, 3H).

¹³C NMR (101 MHz, CD₃OD, major rotamer) δ 173.9, 172.9, 170.4, 159.1, 148.4, 140.2, 138.2, 132.3, 130.4, 129.4, 129.0, 128.8, 122.9, 122.5, 121.3, 118.6, 67.8, 62.5, 47.8, 47.2, 44.2, 35.2, 30.7, 25.9.

HRMS calcd. for C₂₆H₂₉N₆O₆ ([M + H]⁺): 521.2149, found: 521.2178.

(S)-2-(4-(3-(1-(2-(((benzyloxy)carbonyl)amino)acetyl)pyrrolidine-2-carboxamido)phenyl)-1H-1,2,3-triazol-1-yl)acetic acid (RBM7-031)

Compound **RBM7-031** (white solid, 32 mg, 82 %) was obtained from methyl ester **RBM7-027** (40 mg, 0.077 mmol) and LiOH (6 mg, 0.231 mmol), according to general procedure 4.

¹H NMR (400 MHz, CD₃OD, major rotamer) δ 8.28 (s, 1H), 8.00 (t, *J* = 1.8 Hz, 1H), 7.60 – 7.52 (m, 2H), 7.41 – 7.22 (m, 5H), 5.30 (s, 2H), 5.08 (s, 2H), 4.57 (dd, *J* = 8.3, 3.7 Hz, 1H), 4.01 (app q, *J* = 17.1 Hz, 2H), 3.73 – 3.64 (m, 1H), 3.64 – 3.56 (m, 1H), 2.32 – 2.19 (m, 1H), 2.17 – 1.95 (m, 3H).

¹³C NMR (101 MHz, CD₃OD, major rotamer) δ 172.9, 170.4, 169.9, 159.1, 148.6, 140.2, 138.2, 132.3, 130.4, 129.4, 129.0, 128.8, 123.9, 122.5, 121.3, 118.6, 67.8, 62.5, 51.8, 47.8, 44.2, 30.7, 25.9.

HRMS calcd. for C₂₅H₂₇N₆O₆ ([M + H]⁺): 507.1992, found: 507.1996.

2-(4-(3-(2-(2-fluoro-[1,1'-biphenyl]-4-yl)propanamido)phenyl)-1*H*-1,2,3-triazol-1-yl)acetic acid (RBM7-042)

Compound **RBM7-042** (white solid, 27 mg, 56 %) was obtained from methyl ester **RBM7-034** (50 mg, 0.109 mmol) and LiOH (8 mg, 0.327 mmol), according to general procedure 4.

¹H NMR (400 MHz, CD₃OD/CDCl₃ (1:1)) δ 8.15 (s, 1H), 7.93 (t, *J* = 1.8 Hz, 1H), 7.62 (ddd, *J* = 8.1, 2.1, 0.9 Hz, 1H), 7.54 – 7.46 (m, 3H), 7.42 – 7.21 (m, 7H), 5.22 (s, 2H), 3.84 (q, *J* = 7.0 Hz, 1H), 1.57 (d, *J* = 7.0 Hz, 3H).

¹³C NMR (101 MHz, CD₃OD/CDCl₃ (1:1)) δ 174.0, 168.9, 160.3 (d, *J*_{C-F} = 248.5 Hz), 148.2, 143.6 (d, *J*_{C-F} = 7.1 Hz), 139.7, 136.2 (d, *J*_{C-F} = 1.0 Hz), 131.3 (d, *J*_{C-F} = 8.1 Hz), 131.3, 130.0, 129.4 (d, *J*_{C-F} = 3.0 Hz), 128.9, 128.3 (d, *J*_{C-F} = 14.1 Hz), 128.1, 124.0 (d, *J*_{C-F} = 3.0 Hz), 123.0, 122.0, 120.7, 117.8, 115.6 (d, *J*_{C-F} = 24.2 Hz), 51.4, 47.2, 18.9.

HRMS calcd. for C₂₅H₂₂FN₄O₃ ([M + H]⁺): 445.1676, found: 445.1664.

(*S*)-2-(4-(3-(2,6-bis(((benzyloxy)carbonyl)amino)hexanamido)phenyl)-1*H*-1,2,3-triazol-1-yl)acetic acid (RBM7-043)

Compound **RBM7-043** (white solid, 31 mg, 63 %) was obtained from methyl ester **RBM7-035** (50 mg, 0.080 mmol) and LiOH (6 mg, 0.239 mmol), according to general procedure 4.

¹H NMR (400 MHz, CD₃OD/CDCl₃ (1:1)) δ 8.16 (s, 1H), 7.94 (br s, 1H), 7.59 – 7.54 (m, 3H), 7.39 – 7.14 (m, 10H), 5.23 (s, 2H), 5.08 (s, 2H), 5.01 (s, 2H), 4.25 (dd, *J* = 8.1, 5.5 Hz, 1H), 3.12 (t, *J* = 6.5 Hz, 2H), 1.91 – 1.78 (m, 1H), 1.77 – 1.64 (m, 1H), 1.58 – 1.36 (m, 4H).

^{13}C NMR (101 MHz, $\text{CD}_3\text{OD}/\text{CDCl}_3$ (1:1)) δ 172.4, 168.9, 158.1, 157.6, 148.2, 139.2, 137.3, 137.0, 131.4, 130.0, 129.0, 128.9, 128.6, 128.5, 128.4, 128.3, 123.0, 122.2, 120.8, 118.0, 67.5, 67.0, 56.2, 51.4, 40.8, 32.7, 29.8, 23.3.

HRMS calcd. for $\text{C}_{32}\text{H}_{35}\text{N}_6\text{O}_7$ ($[\text{M} + \text{H}]^+$): 615.2567, found: 615.2552.

(S)-2-(4-(3-(2-(((9H-fluoren-9-yl)methoxy)carbonyl)amino)-3-cyclohexylpropanamido)phenyl)-1H-1,2,3-triazol-1-yl)acetic acid (RBM7-044)

Compound **RBM7-044** (white solid, 20 mg, 41 %) was obtained from methyl ester **RBM7-033** (50 mg, 0.082 mmol) and LiOH (6 mg, 0.247 mmol), according to general procedure 4.

^1H NMR (400 MHz, $\text{CD}_3\text{OD}/\text{CDCl}_3$ (1:1)) δ 8.15 (s, 1H), 7.93 (t, $J = 1.8$ Hz, 1H), 7.74 (d, $J = 7.5$ Hz, 2H), 7.65 – 7.53 (m, 4H), 7.40 – 7.32 (m, 3H), 7.27 (app t, $J = 7.4$ Hz, 2H), 5.24 (s, 2H), 4.46 – 4.31 (m, 3H), 4.22 (t, $J = 6.8$ Hz, 1H), 1.82 (br d, $J = 11.8$ Hz, 1H), 1.77 – 1.56 (m, 6H), 1.40 (br s, 1H), 1.32 – 1.09 (m, 3H), 1.04 – 0.88 (m, 2H).

^{13}C NMR (101 MHz, $\text{CD}_3\text{OD}/\text{CDCl}_3$ (1:1)) δ 173.2, 168.9, 157.7, 148.2, 144.5, 144.4, 142.0, 139.3, 131.4, 130.1, 128.3, 127.7, 125.6, 123.1, 122.3, 120.9, 120.5, 118.1, 67.5, 54.3, 51.5, 47.8, 40.5, 34.8, 34.3, 33.0, 27.0, 26.9, 26.7.

HRMS calcd. for $\text{C}_{34}\text{H}_{36}\text{N}_5\text{O}_5$ ($[\text{M} + \text{H}]^+$): 594.2716, found: 594.2716.

(R)-3-(4-(3-(2-(((benzyloxy)carbonyl)amino)-2-phenylacetamido)phenyl)-1H-1,2,3-triazol-1-yl)propanoic acid (RBM7-045)

Compound **RBM7-045** (white solid, 36 mg, 74 %) was obtained from methyl ester **RBM7-038** (50 mg, 0.097 mmol) and LiOH (7 mg, 0.292 mmol), according to general procedure 4.

^1H NMR (400 MHz, $\text{CD}_3\text{OD}/\text{CDCl}_3$ (1:1)) δ 8.10 (s, 1H), 7.89 (br s, 1H), 7.59 – 7.53 (m, 2H), 7.52 – 7.44 (m, 3H), 7.37 – 7.22 (m, 8H), 5.40 (br s, 1H), 5.09 (d, $J = 2.6$ Hz, 2H), 4.67 (t, $J = 6.5$ Hz, 2H), 2.98 (t, $J = 6.5$ Hz, 2H).

^{13}C NMR (101 MHz, $\text{CD}_3\text{OD}/\text{CDCl}_3$ (1:1)) δ 173.1, 170.1, 157.1, 147.8, 139.2, 138.0, 136.9, 131.4, 130.0, 129.4, 129.0, 128.6, 128.4, 127.8, 122.2, 120.7, 117.8, 67.6, 59.9, 46.6, 34.8.

HRMS calcd. for $\text{C}_{27}\text{H}_{26}\text{N}_5\text{O}_5$ ($[\text{M} + \text{H}]^+$): 500.1934, found: 500.1917.

(R)-3-(4-(3-(2-(((benzyloxy)carbonyl)amino)-2-cyclohexylacetamido)phenyl)-1H-1,2,3-triazol-1-yl)propanoic acid (RBM7-046)

Compound **RBM7-046** (white solid, 21 mg, 43 %) was obtained from methyl ester **RBM7-039** (50 mg, 0.096 mmol) and LiOH (7 mg, 0.289 mmol), according to general procedure 4.

¹H NMR (400 MHz, CD₃OD/CDCl₃ (1:1)) δ 8.15 (s, 1H), 7.92 (br s, 1H), 7.61 – 7.56 (m, 1H), 7.54 – 7.50 (m, 1H), 7.39 – 7.16 (m, 6H), 5.08 (s, 2H), 4.69 (t, *J* = 6.5 Hz, 2H), 4.10 (d, *J* = 7.1 Hz, 1H), 2.99 (t, *J* = 6.5 Hz, 2H), 1.83 – 1.61 (m, 6H), 1.28 – 1.03 (m, 5H).

¹³C NMR (101 MHz, CD₃OD/CDCl₃ (1:1)) δ 173.1, 171.9, 157.7, 147.9, 139.1, 137.1, 131.4, 130.1, 129.0, 128.6, 128.4, 122.2, 120.8, 117.9, 67.5, 61.3, 46.6, 41.5, 34.8, 30.3, 29.2, 26.6, 26.5, 26.5.

HRMS calcd. for C₂₇H₃₂N₅O₅ ([M + H]⁺): 506.2403, found: 506.2391.

2-(4-(3-(1-((benzyloxy)carbonyl)piperidine-3-carboxamido)phenyl)-1H-1,2,3-triazol-1-yl)acetic acid (RBM7-047)

Compound **RBM7-047** (white solid, 20 mg, 41 %) was obtained from methyl ester **RBM7-041** (50 mg, 0.105 mmol) and LiOH (8 mg, 0.314 mmol), according to general procedure 4.

¹H NMR (400 MHz, CD₃OD/CDCl₃ (1:1)) δ 8.15 (s, 1H), 7.90 (br s, 1H), 7.59 (br d, *J* = 7.6 Hz, 1H), 7.52 (br d, *J* = 7.6 Hz, 1H), 7.39 – 7.22 (m, 6H), 5.23 (s, 2H), 5.15 – 5.06 (m, 2H), 4.28 – 4.21 (m, 1H), 4.10 (app d, *J* = 13.0 Hz, 1H), 3.06 (br s, 1H), 2.88 (br s, 1H), 2.50 (tt, *J* = 11.0, 3.7 Hz, 1H), 2.05 (br d, *J* = 10.8 Hz, 1H), 1.86 – 1.70 (m, 2H), 1.59 – 1.43 (m, 1H).

¹³C NMR (101 MHz, CD₃OD/CDCl₃ (1:1)) δ 174.0, 169.4, 156.7, 148.5, 140.0, 137.6, 131.9, 130.3, 129.3, 128.9, 128.6, 123.5, 122.3, 120.9, 118.1, 68.2, 51.6, 47.3, 45.1 (br), 44.7, 28.8 (br), 25.4 (br).

HRMS calcd. for C₂₄H₂₆N₅O₅ ([M + H]⁺): 464.1934, found: 464.1924.

(R)-3-(4-(3-(2-(((benzyloxy)carbonyl)amino)-3-(4-hydroxyphenyl)propanamido)phenyl)-1H-1,2,3-triazol-1-yl)propanoic acid (RBM7-048)

Compound **RBM7-048** (white solid, 19 mg, 39 %) was obtained from methyl ester **RBM7-040** (50 mg, 0.092 mmol) and LiOH (7 mg, 0.276 mmol), according to general procedure 4.

¹H NMR (400 MHz, CD₃OD/CDCl₃ (1:1)) δ 8.11 (s, 1H), 7.78 (br s, 1H), 7.54 – 7.51 (m, 1H), 7.49 (ddd, *J* = 8.1, 2.1, 1.1 Hz, 1H), 7.37 – 7.16 (m, 6H), 7.04 (d, *J* = 8.5 Hz, 2H), 6.73 – 6.68 (m, 2H), 5.05 (d, *J* = 11.4 Hz, 2H, major rotamer), 4.68 (t, *J* = 6.5 Hz, 2H), 4.46 (t, *J* =

7.0 Hz, 1H), 3.05 (dd, $J = 13.7, 6.7$ Hz, 1H), 2.99 (t, $J = 6.5$ Hz, 2H), 2.91 (dd, $J = 13.6, 7.6$ Hz, 1H).

^{13}C NMR (101 MHz, $\text{CD}_3\text{OD}/\text{CDCl}_3$ (1:1)) δ 173.1, 171.7, 157.3, 156.4, 147.8, 139.0, 137.0, 131.4, 130.9, 130.0, 129.0, 128.6, 128.3, 127.9, 122.3, 122.2, 120.9, 118.1, 115.9, 67.4, 57.8, 46.6, 38.5, 34.8.

HRMS calcd. for $\text{C}_{28}\text{H}_{28}\text{N}_5\text{O}_6$ ($[\text{M} + \text{H}]^+$): 530.2040, found: 530.2048.

3-(4-(3-(2-hydroxy-2-(4-hydroxy-3-methoxyphenyl)acetamido)phenyl)-1H-1,2,3-triazol-1-yl)propanoic acid (RBM7-049)

Compound **RBM7-049** (white solid, 59 mg, 91 %) was obtained from methyl ester **RBM7-037** (67 mg, 0.157 mmol) and LiOH (11 mg, 0.471 mmol), according to general procedure 4. Once evaporated, the crude reaction mixture was dissolved in DMSO/ H_2O (1:1) and loaded on an Amberlite XAD-4 column (5 g), which had been washed thoroughly with acetone and then equilibrated with water. Elution with a linear gradient from 0 to 40 % MeCN in H_2O provided pure **RBM7-049**.

^1H NMR (400 MHz, $\text{CD}_3\text{OD}/\text{CDCl}_3$ (1:1)) δ 8.13 (s, 1H), 7.95 (t, $J = 1.8$ Hz, 1H), 7.61 (ddd, $J = 8.1, 2.1, 1.0$ Hz, 1H), 7.56 – 7.52 (m, 1H), 7.37 (t, $J = 7.9$ Hz, 1H), 7.04 (d, $J = 2.0$ Hz, 1H), 6.95 (dd, $J = 8.2, 2.0$ Hz, 1H), 6.80 (d, $J = 8.1$ Hz, 1H), 5.08 (s, 1H), 4.68 (t, $J = 6.5$ Hz, 2H), 3.86 (s, 3H), 2.98 (t, $J = 6.5$ Hz, 2H).

^{13}C NMR (101 MHz, $\text{CD}_3\text{OD}/\text{CDCl}_3$ (1:1)) δ 173.2 (br), 173.0, 148.2, 147.8, 146.8, 138.7, 131.9, 131.5, 130.1, 122.3, 122.2, 120.6, 120.2, 117.9, 115.5, 110.6, 74.9, 56.1, 46.6, 34.9.

HRMS calcd. for $\text{C}_{20}\text{H}_{21}\text{N}_4\text{O}_6$ ($[\text{M} + \text{H}]^+$): 413.1461, found: 413.1473.

3-(4-(3-benzamidophenyl)-1H-1,2,3-triazol-1-yl)propanoic acid (RBM7-066)

Compound **RBM7-066** (white solid, 111 mg, 93 %) was obtained from methyl ester **RBM7-065** (125 mg, 0.357 mmol) and LiOH (26 mg, 1.07 mmol) in THF/ H_2O (3:1) (50 ml), according to general procedure 4.

^1H NMR (400 MHz, CD_3OD) δ 8.33 (s, 1H), 8.12 (t, $J = 1.8$ Hz, 1H), 7.98 – 7.94 (m, 2H), 7.73 (ddd, $J = 8.1, 2.1, 1.0$ Hz, 1H), 7.63 – 7.56 (m, 2H), 7.56 – 7.50 (m, 2H), 7.44 (t, $J = 7.9$ Hz, 1H), 4.72 (t, $J = 6.6$ Hz, 2H), 3.02 (t, $J = 6.6$ Hz, 2H).

^{13}C NMR (101 MHz, $\text{CD}_3\text{OD}/\text{CDCl}_3$ (1:1)) δ 173.6, 168.6, 148.1, 140.0, 135.7, 132.6, 131.7, 130.2, 129.2, 128.3, 122.5, 122.5, 121.8, 118.9, 46.9, 35.1.

HRMS calcd. for $\text{C}_{18}\text{H}_{17}\text{N}_4\text{O}_3$ ($[\text{M} + \text{H}]^+$): 337.1301, found: 337.1299.

3-(4-(3-(2-phenylacetamido)phenyl)-1*H*-1,2,3-triazol-1-yl)propanoic acid (RBM7-067)

Compound **RBM7-067** (white solid, 114 mg, 79 %) was obtained from methyl ester **RBM7-54** (150 mg, 0.412 mmol) and LiOH (30 mg, 1.23 mmol) in THF/ H_2O (3:1) (50 ml), according to general procedure 4.

^1H NMR (400 MHz, $\text{CD}_3\text{OD}/\text{CDCl}_3$ (1:1)) δ 8.12 (s, 1H), 7.88 (t, $J = 1.8$ Hz, 1H), 7.60 (ddd, $J = 8.1, 2.1, 1.0$ Hz, 1H), 7.52 – 7.48 (m, 1H), 7.37 – 7.28 (m, 5H), 7.26 – 7.20 (m, 1H), 4.67 (t, $J = 6.5$ Hz, 2H), 3.68 (s, 2H), 2.98 (t, $J = 6.5$ Hz, 2H).

^{13}C NMR (101 MHz, $\text{CD}_3\text{OD}/\text{CDCl}_3$ (1:1)) δ 173.2, 171.6, 147.9, 139.6, 135.7, 131.3, 130.0, 129.6, 129.1, 127.5, 122.1, 122.0, 120.6, 117.7, 46.6, 44.4, 34.9.

HRMS calcd. for $\text{C}_{19}\text{H}_{19}\text{N}_4\text{O}_3$ ($[\text{M} + \text{H}]^+$): 351.1457, found: 351.1454.

Fluorogenic assay of S1PL enzyme activity

Recombinant bacterial or human S1PL (50 μL from stock solutions in buffer A (StS1PL) or B (hS1PL), final concentration: 25 $\mu\text{g}/\text{mL}$ for StS1PL and 3 $\mu\text{g}/\text{mL}$ for hS1PL) was added to a mixture of **RBM13** (added from a stock solution in 0.5 M potassium phosphate buffer, pH 7.2; final concentration: 125 μM .) and putative inhibitors (added from stock solutions in DMSO; final DMSO: 2.5 %) in either buffer solution A (StS1PL) or B (hS1PL) (final volume: 100 μL). Buffer solution A correspond to a 1 mM potassium phosphate buffer, pH 7.2, containing 100 mM NaCl, 1 mM EDTA, 1 mM DTT, 10 μM pyridoxal 5'-phosphate. Buffer solution B correspond to a 100 mM HEPES buffer, pH 7.4, containing 0.1 mM EDTA, 0.05 % Triton X-100, 0.01 % Pluronic F127 (Biotium), and 100 μM pyridoxal 5'-phosphate. The mixture was incubated at 37 $^\circ\text{C}$ for 1 h and the enzymatic reaction was stopped by the addition of 50 μL of MeOH. Finally, 100 μL of a 200 mM glycine-NaOH buffer, pH 10.6, were added to the resulting solution and the mixture was incubated for 20 additional min at 37 $^\circ\text{C}$ in order to complete the β -elimination reaction. The amount of umbelliferone formed was determined on either a SpectraMax M5 (Molecular Devices) or Synergy 2 (BioTek)

microplate readers ($\lambda_{\text{ex/em}} = 355/460 \text{ nm}$), using a calibration curve. V_{max} and K_{M} values were determined by measuring initial velocities at different **RBM13** concentrations and fitting the data to the Michaelis–Menten equation in Prism 5 (GraphPad Software, La Jolla). IC_{50} values were determined by plotting percent activity versus $\log [I]$ and fitting the data to the $\log(\text{inhibitor})$ vs. response equation in Prism 5 (GraphPad Software, La Jolla). In both cases, settings for curve adjustments were kept with their default values.

LC/MS assay of S1PL enzyme activity

Recombinant bacterial or human S1PL (50 μL from stock solutions in buffer B; final concentration: 0.8 $\mu\text{g/mL}$) was added to a mixture of S1P (added from a stock solution in 1 % aq. Triton X-100; final concentration: 10 μM), and compound D (added from a stock solution in DMSO; final concentration: 50 μM ; final DMSO: 2.5 %) in buffer solution B (final volume: 100 μL). The reaction mixture was incubated at 37 $^{\circ}\text{C}$ for 1 h and stopped by the successive addition of pentadecenal (5 μL ; final concentration: 3.7 μM) and isoniazid (95 μL ; final concentration: 3.1 mM) stock solutions in ACN/300 mM aq. H_2SO_4 (1:1). Samples were analyzed using a Waters Acquity UPLC system connected to a Waters LCT Premier Orthogonal Accelerated Time of Flight Mass Spectrometer (Waters, Millford, MA), operated in positive electrospray ionization mode. Full scan spectra from 50 to 1500 Da were obtained. Mass accuracy and reproducibility were maintained by using an independent reference spray via LockSpray. A 100 mm x 2.1 mm id, 1.7 mm C18 Acquity UPLC BEH (Waters) analytical column was used. The two mobile phases were acetonitrile (phase A) and water (phase B), both phases with 0.2% of formic acid. The linear gradient was: 0 min, 90% B; 5 min, 100% A; 6.5 min, 100% A; 7.2 min, 90% B and 8 min, 90% B at 0.3 ml/min. The column was held at 30 $^{\circ}\text{C}$. Positive identification of compounds was based on the accurate mass measurement with an error <5 ppm and its LC retention time calculated with authentic 2EC16-ISO and C15-ISO standards. Exact masses ($[\text{M}+\text{H}]^+$) of both (*E*)-*N'*-[(*E*)-hexadec-2-en-1-ylidene]isonicotinohydrazide (2EC16-ISO) and (*E*)-*N'*-(1-pentadecylidene)isonicotinohydrazide (C15-ISO) (m/z : 358.2858 and 346.2858, respectively) were extracted from TIC chromatograms and the area of the resulting peaks was calculated using MassLynx. The area ratio between 2EC16-ISO and C15-ISO was used as a measure of S1PL activity.

References

- (1) Bandhuvula, P.; Saba, J. D. Sphingosine-1-Phosphate Lyase in Immunity and Cancer: Silencing the Siren. *Trends Mol. Med.* **2007**, *13* (5), 210–217.
- (2) Spiegel, S.; Milstien, S. Sphingosine-1-Phosphate: An Enigmatic Signalling Lipid. *Nat Rev Mol Cell Biol* **2003**, *4* (5), 397–407.
- (3) Newton, J.; Lima, S.; Maceyka, M.; Spiegel, S. Revisiting the Sphingolipid Rheostat: Evolving Concepts in Cancer Therapy. *Exp. Cell Res.* **2015**, *333* (2), 195–200.
- (4) Schwab, S. R.; Pereira, J. P.; Matloubian, M.; Xu, Y.; Huang, Y.; Cyster, J. G. Lymphocyte Sequestration through S1P Lyase Inhibition and Disruption of S1P Gradients. *Science* **2005**, *309* (5741), 1735–1739.
- (5) Van Veldhoven, P. P. Sphingosine-1-Phosphate Lyase. *Methods Enzymol.* **2000**, *311*, 244–254.
- (6) Bagdanoff, J. T.; Donoviel, M. S.; Nouraldeen, A.; Tarver, J.; Fu, Q.; Carlsen, M.; Jessop, T. C.; Zhang, H.; Hazelwood, J.; Nguyen, H.; Baugh, S. D.; Gardyan, M.; Terranova, K. M.; Barbosa, J.; Yan, J.; Bednarz, M.; Layek, S.; Courtney, L. F.; Taylor, J.; Digeorge-Foushee, A. M.; Gopinathan, S.; Bruce, D.; Smith, T.; Moran, L.; O'Neill, E.; Kramer, J.; Lai, Z.; Kimball, S. D.; Liu, Q.; Sun, W.; Yu, S.; Swaffield, J.; Wilson, A.; Main, A.; Carson, K. G.; Oravec, T.; Augeri, D. J. Inhibition of Sphingosine-1-Phosphate Lyase for the Treatment of Autoimmune Disorders. *J Med Chem* **2009**, *52* (13), 3941–3953.
- (7) Bagdanoff, J. T.; Donoviel, M. S.; Nouraldeen, A.; Carlsen, M.; Jessop, T. C.; Tarver, J.; Aleem, S.; Dong, L.; Zhang, H.; Boteju, L.; Hazelwood, J.; Yan, J.; Bednarz, M.; Layek, S.; Owusu, I. B.; Gopinathan, S.; Moran, L.; Lai, Z.; Kramer, J.; Kimball, S. D.; Yalamanchili, P.; Heydorn, W. E.; Frazier, K. S.; Brooks, B.; Brown, P.; Wilson, A.; Sonnenburg, W. K.; Main, A.; Carson, K. G.; Oravec, T.; Augeri, D. J. Inhibition of Sphingosine 1-Phosphate Lyase for the Treatment of Rheumatoid Arthritis: Discovery of (E)-1-(4-((1 R,2 S,3 R)-1,2,3,4-Tetrahydroxybutyl)-1 H -Imidazol-2-Yl)ethanone Oxime (LX2931) and (1 R,2 S,3 R)-1-(2-(Isoxazol-3-Yl)-1 H -Imidazol-4-Yl)but. *J. Med. Chem.* **2010**, *53*, 8650–8662.
- (8) Bigaud, M.; Guerini, D.; Billich, A.; Bassilana, F.; Brinkmann, V. Second Generation S1P Pathway Modulators: Research Strategies and Clinical Developments. *Biochim. Biophys. Acta* **2014**, *1841* (5), 745–758.
- (9) Stoffel, W.; Grol, M. Chemistry and Biochemistry of 1-Desoxysphinganine-1-Phosphonate (Dihydrosphingosine-1-Phosphonate). *Chem. Phys. Lipids* **1974**, *13*, 372–388.

- (10) Bandhuvula, P.; Tam, Y. Y.; Oskouian, B.; Saba, J. D. The Immune Modulator FTY720 Inhibits Sphingosine-1-Phosphate Lyase Activity. *J. Biol. Chem.* **2005**, *280*, 33697–33700.
- (11) Berdyshev, E. V.; Goya, J.; Gorshkova, I.; Prestwich, G. D.; Byun, H. S.; Bittman, R.; Natarajan, V. Characterization of Sphingosine-1-Phosphate Lyase Activity by Electrospray Ionization-Liquid Chromatography/tandem Mass Spectrometry Quantitation of (2E)-Hexadecenal. *Anal Biochem* **2011**, 12–18.
- (12) Brinkmann, V.; Billich, A.; Baumruker, T.; Heining, P.; Schmouder, R.; Francis, G.; Aradhya, S.; Burtin, P. Fingolimod (FTY720): Discovery and Development of an Oral Drug to Treat Multiple Sclerosis. *Nat Rev Drug Discov* **2010**, *9* (11), 883–897.
- (13) Kashem, M. A.; Wa, C.; Wolak, J. P.; Grafos, N. S.; Ryan, K. R.; Sanville-Ross, M. L.; Fogarty, K. E.; Rybina, I. V.; Shoultz, A.; Molinaro, T.; Desai, S. N.; Rajan, A.; Huber, J. D.; Nelson, R. M. A High-Throughput Scintillation Proximity Assay for Sphingosine-1-Phosphate Lyase. *Assay Drug Dev. Technol.* **2014**, *12* (5), 1–10.
- (14) Loetscher, E.; Schneider, K.; Beerli, C.; Billich, A. Assay to Measure the Secretion of Sphingosine-1-Phosphate from Cells Induced by S1P Lyase Inhibitors. *Biochem Biophys Res Commun* **2013**, *433* (3), 345–348.
- (15) Weiler, S.; Braendlin, N.; Beerli, C.; Bergsdorf, C.; Schubart, A.; Srinivas, H.; Oberhauser, B.; Billich, A. Orally Active 7-Substituted (4-Benzyl-Phthalazin-1-Yl)-2-Methyl-Piperazin-1-Yl-Nicotinonitriles as Active-Site Inhibitors of Sphingosine-1-Phosphate Lyase for the Treatment of Multiple Sclerosis. *J. Med. Chem.* **2014**, *57* (12), 5074–5084.
- (16) Dinges, J.; Harris, C. M.; Wallace, G. A.; Argiriadi, M. A.; Queeney, K. L.; Perron, D. C.; Dominguez, E.; Kebede, T.; Desino, K. E.; Patel, H.; Vasudevan, A. Hit-to-Lead Evaluation of a Novel Class of Sphingosine 1-Phosphate Lyase Inhibitors. *Bioorg. Med. Chem. Lett.* **2016**, DOI: 10.1016/j.bmcl.2016.03.043.
- (17) Deniz, U.; Ozkirimli, E.; Ulgen, K. O. A Systematic Methodology for Large Scale Compound Screening: A Case Study on the Discovery of Novel S1PL Inhibitors. *J. Mol. Graph. Model.* **2016**, *63*, 110–124.
- (18) Ikeda, M.; Kihara, A.; Igarashi, Y. Sphingosine-1-Phosphate Lyase SPL Is an Endoplasmic Reticulum-Resident, Integral Membrane Protein with the Pyridoxal 5'-phosphate Binding Domain Exposed to the Cytosol. *Biochem. Biophys. Res. Commun.* **2004**, *325* (1), 338–343.
- (19) Bourquin, F.; Riezman, H.; Capitani, G.; Grutter, M. G. Structure and Function of Sphingosine-1-Phosphate Lyase, a Key Enzyme of Sphingolipid Metabolism. *Structure* **2010**, *18* (8), 1054–1065.
- (20) Pulkoski-Gross, M. J.; Donaldson, J. C.; Obeid, L. M. Sphingosine-1-Phosphate Metabolism: A Structural Perspective. *Crit. Rev. Biochem. Mol. Biol.* **2015**, *50* (4),

298–313.

- (21) Van Veldhoven, P. P.; Gijsbers, S.; Mannaerts, G. P.; Vermeesch, J. R.; Brys, V. Human Sphingosine-1-Phosphate Lyase: cDNA Cloning, Functional Expression Studies and Mapping to Chromosome 10q22(1). *Biochim. Biophys. Acta* **2000**, *1487* (2-3), 128–134.
- (22) Bedia, C.; Camacho, L.; Casas, J.; Abad, J. L.; Delgado, A.; Van Veldhoven, P. R.; Fabrias, G. Synthesis of a Fluorogenic Analogue of Sphingosine-1-Phosphate and Its Use to Determine Sphingosine-1-Phosphate Lyase Activity. *ChemBioChem* **2009**, *10* (5), 820–822.
- (23) MOE Leadlike Database, v. 2011.10. Chemical Computing Group Inc.: Montreal, QC, Canada, 2011.
- (24) Schrödinger Virtual Screening Workflow 2015-2. Schrödinger, LLC: New York, NY, 2015.
- (25) Schrödinger Glide, Version 6.7, Schrödinger, LLC, New York, NY, 2015.
- (26) Halgren, T. A.; Murphy, R. B.; Friesner, R. A.; Beard, H. S.; Frye, L. L.; Pollard, W. T.; Banks, J. L. Glide: A New Approach for Rapid, Accurate Docking and Scoring. 2. Enrichment Factors in Database Screening. *J Med Chem* **2004**, *47* (7), 1750–1759.
- (27) Friesner, R. A.; Murphy, R. B.; Repasky, M. P.; Frye, L. L.; Greenwood, J. R.; Halgren, T. A.; Sanschagrin, P. C.; Mainz, D. T. Extra Precision Glide: Docking and Scoring Incorporating a Model of Hydrophobic Enclosure for Protein-Ligand Complexes. *J Med Chem* **2006**, *49* (21), 6177–6196.
- (28) Friesner, R. A.; Banks, J. L.; Murphy, R. B.; Halgren, T. A.; Klicic, J. J.; Mainz, D. T.; Repasky, M. P.; Knoll, E. H.; Shelley, M.; Perry, J. K.; Shaw, D. E.; Francis, P.; Shenkin, P. S. Glide: A New Approach for Rapid, Accurate Docking and Scoring. 1. Method and Assessment of Docking Accuracy. *J Med Chem* **2004**, *47* (7), 1739–1749.
- (29) Elliott, T. S.; Slowey, A.; Ye, Y.; Conway, S. J. The Use of Phosphate Bioisosteres in Medicinal Chemistry and Chemical Biology. *Medchemcomm* **2012**, *3* (7), 735–751.
- (30) Schrödinger Induced Fit Docking Protocol 2015-2, Schrödinger LCC: New York, NY, 2015.
- (31) Sherman, W.; Beard, H. S.; Farid, R. Use of an Induced Fit Receptor Structure in Virtual Screening. *Chem. Biol. Drug Des.* **2006**, *67* (1), 83–84.
- (32) Sherman, W.; Day, T.; Jacobson, M. P.; Friesner, R. A.; Farid, R. Novel Procedure for Modeling Ligand/receptor Induced Fit Effects. *J. Med. Chem.* **2006**, *49* (2), 534–553.
- (33) Nieves, I.; Sanllehi, P.; Abad, J.-L. L.; Fabrias, G.; Casas, J.; Delgado, A.; Fabriás, G.; Casas, J.; Delgado, A. Chemical Probes of Sphingolipid Metabolizing Enzymes. In *Bioactive Sphingolipid in Cancer Biology and Therapy*; Hannun, Y., Luberto, C.,

- Obeid, L., Mao, C., Eds.; Springer International Publishing: Switzerland, 2015; pp 437–469.
- (34) Reina, E.; Camacho, L.; Casas, J.; Van Veldhoven, P. P.; Fabrias, G. Determination of Sphingosine-1-Phosphate Lyase Activity by Gas Chromatography Coupled to Electron Impact Mass Spectrometry. *Chem. Phys. Lipids* **2012**, *165* (2), 225–231.
- (35) Argiriadi, M. A.; Banach, D.; Radziejewska, E.; Marchie, S.; DiMauro, J.; Dinges, J.; Dominguez, E.; Hutchins, C.; Judge, R. A.; Queeney, K.; Wallace, G.; Harris, C. M. Creation of a S1P Lyase Bacterial Surrogate for Structure-Based Drug Design. *Bioorg. Med. Chem. Lett.* **2016**, DOI: 10.1016/j.bmcl.2016.02.084.
- (36) Nervall, M.; Hanspers, P.; Carlsson, J.; Boukharta, L.; Aqvist, J. Predicting Binding Modes from Free Energy Calculations. *J. Med. Chem.* **2008**, *51* (9), 2657–2667.
- (37) Unpublished Results from Our Group.
- (38) Szulc, Z. M.; Hannun, Y. A.; Bielawska, A. A Facile Regioselective Synthesis of Sphingosine 1-Phosphate and Ceramide 1-Phosphate. *Tetrahedron Lett.* **2000**, *41* (41), 7821–7824.
- (39) Sbardella, G.; Castellano, S.; Vicidomini, C.; Rotili, D.; Nebbioso, A.; Miceli, M.; Altucci, L.; Mai, A. Identification of Long Chain Alkylidenemalonates as Novel Small Molecule Modulators of Histone Acetyltransferases. *Bioorg. Med. Chem. Lett.* **2008**, *18* (9), 2788–2792.

Graphical Abstract

